Evrimata: Journal of Mechanical Engineering
Vol. 01, No. 04, December, 2024, p. 108 – 117 e-ISSN: 3047-6305

Analysis of The Application of 3D Printing To Design A Water Thruster Jet Boat

Lazuardi Lazuardi [1]✉, Maryono Maryono[2], Sugeng Hadi Susilo[3] Muhammad Akhlis Rizza[4]

[1]Faculty of engineering and science, PGRI Wiranegara University Pasuruan, Indonesia
[2] Malang Army Polytechnic, Indonesia
[3,4] State Polytechnic of Malang, Indonesia

Atingthok99@gmail.com, maryono250375@gmail.com, sugeng.hadi@polinema.ac.id, muh.akhlis@polinema.ac.id

Article Information

Manuscript Received 2024-11-02
Manuscript Revised 2024-12-29
Manuscript Accepted 2024-12-29
Manuscript Online 2024-12-31

ABSTRACT

This study explores the use of 3D printing technology to design and manufacture water thrusters for jet boats, overcoming challenges in traditional manufacturing such as high costs, limited customization, and long production times. The main components of the water thruster are made of ABS (Acrylonitrile Butadiene Styrene) filament material and the performance of the water thruster for jet boats is tested using CFD (Computational Fluid Dynamics) simulation. The results show that the 3D printed ABS filament can be used as an impeller component with a maximum tensile strength of 24 Mpa which is declared safe because the maximum stress that occurs in the impeller when working is 18.73 Mpa. The analysis of the performance of the resulting water jet propulsion reached 571 cm/s which showed increased efficiency and operational stability. showed that the 3D printed water for jet boats offers comparable performance to conventionally manufactured systems while reducing costs and production times. In addition, 3D printing has proven effective in offering innovative solutions that have the potential to improve the performance and efficiency of the maritime industry.

Keywords: 3D printing, water thruster jet, impeller design optimization, additive manufacturing technology.

1. INTRODUCTION

3D printing, or additive manufacturing, is a technology used to print three-dimensional objects from digital models. The technology works by gradually adding material layer by layer based on a design that has been generated using computer-aided design (CAD) software. One of the main advantages of 3D printing is its ability to create complex geometric shapes that are difficult or impossible to create using traditional manufacturing methods [1]. 3D printing is widely applied in various industries, including automotive, healthcare, and aerospace, especially in the manufacture of prototypes and spare parts [2]. The materials used in the 3D printing process vary, from plastic to metal, depending on the specific application [3]. With its rapid growth, this technology is considered one of the innovations that is changing the global manufacturing ecosystem [4], accelerating production processes, and reducing product development costs [5].

Water thruster jet is a propulsion device used to move boats or ships by utilizing water thrust. This system works by sucking water from under the ship and then pumping it out at high pressure through a nozzle, producing forward thrust [6]. This technology offers several advantages over conventional propulsion systems, such as propellers, because it is able to provide better maneuverability at low speeds and is safer for the environment around the ship [7]. In addition, water thruster jets tend to be more efficient in reducing underwater resistance and improving ship performance in shallow waters [8]. This system is widely used in fast boats, military ships, and jet skis because of its more responsive speed and maneuverability [9]. Recent developments in jet nozzle materials and designs have also increased the efficiency and durability of this propulsion system [10].

The efficiency of water thruster jets makes them an increasingly popular propulsion solution in the modern maritime industry. This system works by converting mechanical energy into water thrust that propels the vessel forward by utilizing nozzles designed to generate high pressure [11][12]. The main advantages of this technology are its efficiency in reducing underwater drag, increasing vessel speed, and better maneuverability compared to conventional propellers, especially in shallow waters [13]. In addition, water thruster jets are also safer for the environment because they reduce the risk of damage to underwater ecosystems, such as coral reefs [14][15]. In practical applications, this system can be optimized for various sizes of vessels, from jet skis to naval vessels, and is more fuel efficient due to better water flow efficiency

[16]. Recent research has shown improvements in nozzle design and materials, which contribute to durability and long-term performance [17].

The optimization of the design of the water thruster jet boat aims to improve the propulsion efficiency, speed, and maneuverability of the ship. One important aspect in this optimization is the development of the nozzle design to maximize water flow and reduce turbulence, resulting in greater thrust with lower energy consumption [18]. The use of lighter and corrosion-resistant materials, such as aluminum alloys and carbon fiber composites, is also a focus to increase durability and reduce the overall weight of the system [19]. In addition, hydrodynamic simulations using Computational Fluid Dynamics (CFD) are used to analyze and improve the water flow pattern around the thruster, improving overall performance [20][21]. Research also shows that a more efficient internal propeller design can reduce fuel consumption and increase acceleration [22]. Automatic control technology on jet thrusters also allows ships to maneuver with more precision [23].

The construction of water jet thrusters is optimized to ensure adequate durability and strength. Lightweight yet strong materials such as ABS (Acrylonitrile Butadiene Styrene) filaments are often chosen because they can be printed using 3D printing technology, making it easier to manufacture complex components [24][25]. This material has properties that are resistant to impact, corrosion, and can operate in harsh marine environments [26]. The use of 3D printing allows engineers to create more precise and complex designs at lower costs and faster production times [27]. In addition, 3D printing also opens up the possibility of producing prototypes efficiently and performing design iterations to optimize thruster performance [28]. The selection of materials such as ABS can also reduce the total weight of the propulsion system, increase the fuel efficiency of the ship, and extend the operational life of the device [29].

Additive manufacturing, or 3D printing, opens up new opportunities for innovation in the design and production of water jet boat thrusters. This technology allows for the creation of components with complex geometries and lightweight, which are difficult to achieve through traditional manufacturing methods [30]. With additive manufacturing, designers can easily prototype jet thrusters in less time and at lower costs, while maintaining quality and performance [31]. Materials such as alloys and ABS polymers are widely used to print thruster components due to their durability and strength under marine operating conditions [32]. In addition, additive manufacturing's ability to produce lightweight yet strong internal structures helps improve fuel efficiency and overall boat performance [33]. This technology also facilitates innovation in more aerodynamic nozzle designs, increasing thrust while reducing water resistance [34].

2. RESEARCH SIGNIFICANCE

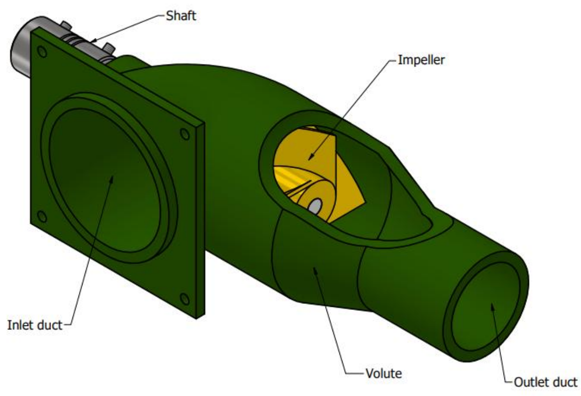

Fig 1 planned water thruster jet boat. planned water thruster jet boat.

Innovations in additive manufacturing technology allow for rapid design testing and adjustment, accelerating the development process. With proper optimization, water thruster jet boats can achieve high performance with better fuel efficiency, increased maneuverability, and shallow water operation capabilities, making them an ideal choice for a variety of maritime applications. From the planned design of the water thruster jet boat, the performance specifications of the water thruster are obtained, as presented in Table 1. As follows:

Table 1. Water thruster jet performance specifications

Water thruster jet performance	
Shaft	Logam stailistel (Ø 5 mm)
Impeller	4 Road (1500 rpm)
Inlet Duct	Inlet Ø 39 mm
Volute	3.06 m/s
Outlet Duct	Outlet Ø 24 mm

From the planned water thruster jet boat design, a detailed drawing can be explained showing the complete dimensions of the pump body water thruster jet. can be seen in Fig 2 as follows:

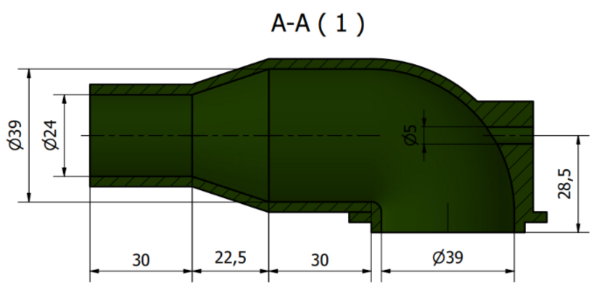

Fig 2 . Water thruster jet pump body dimensions.

From the planned jet boat water thruster design, the water thruster impeller specifications are obtained, which are presented in Table 2. As follows:

Table 2. Water thruster jet impeller specifications

impeller water thruster jet	
Tip	Ø 39 mm
Boss	Ø 15 mm length 15 mm
Propeller Shaft	Ø 5 mm length 70 mm
Leading Edge	Angle 36˚
Root	4 propellers
Trailing Edge	Angle 36˚
Propeller Axis	Horizontal axis

Table 2, it can be explained the impeller image that displays the complete parts of the water thruster jet impeller. can be seen in Fig 3 as follows:

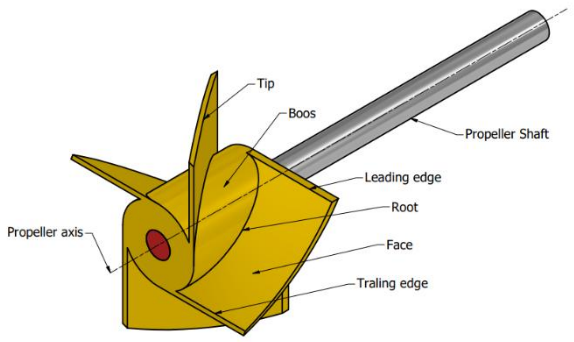

Fig 3 . Water thruster jet impeller parts.

To engineer the results of a strong water thruster jet print, researchers use a combination of 3D printing parameters with a 3D printing parameter formula of 0.1mm layer height, 30% gyroid infill, with a speed of 40mm/s. With the analysis of the road impeller angle of 36.6◦ degrees and a combination of 10 mm, 15mm and 20 mm impeller rake lengths. It is hoped that the study will find the right dimensional parameters to design a strong water thruster jet impeller against water pressure/water hammer.

3. RESEARCH METHODS.

In the 3D printing process of the planned water thruster jet using a 3D printing machine with the Ender 3 Professional brand type, a product of the Shenzhen Creality 3D Technology company, JinChengYuan, China. The machine specifications can be presented in Table 3 showing the specifications of the Ender 3 Professional machine.

Table 3. Ender 3 Professional Specifications.

Parameters	Value
Model Number	Ender 3 Pro
Build Size	220*220*250mm
Machine Size	440*440*465mm

The filament material used to print the planned water thruster jet is the ABS (acrylonitrile butadiene styrene) polymer type, Sunlu brand, a product of Zhuhai Sunlu Industrial, Guangdong, China. Table 4 shows the recommended 3D printing temperature standards from the company.

Table 4. ABS Filament Material Specifications.

Recommended Temperature For ABS Filament	
Heated bed (°C)	95-110
Extruder Temperature (°C)	220-250

Mechanical test method and design simulation are used to design the planned water thruster jet design. This method is more effective to find out the relationship between Root angle and Rake length to the mechanical strength of the planned water thruster jet. Fig 6 explains the scheme in this planning:

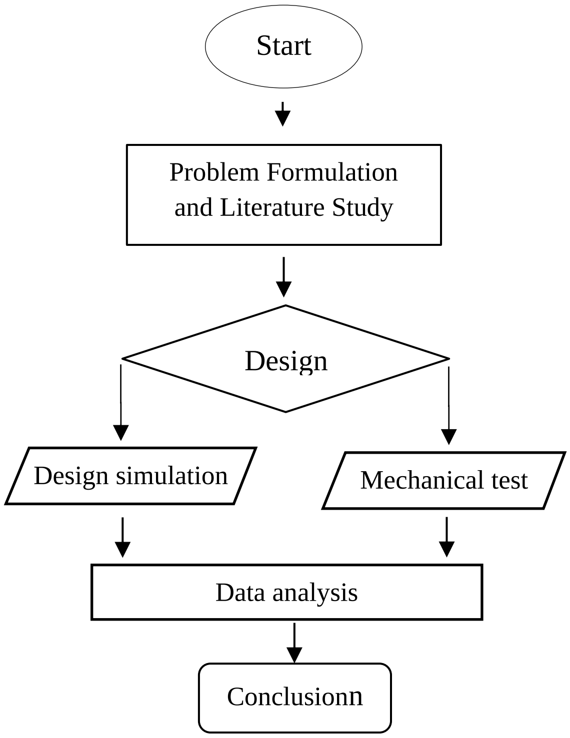

Fig 6. Schematic of the research flow.

Tensile test specimens to determine the mechanical strength of ABS (acrylonitrile butadiene styrene) filament material using the JIS Z2201 standard [Hadi S: 2016]. Fig 7 explains the standard size of the JIS Z2201 tensile test specimen.

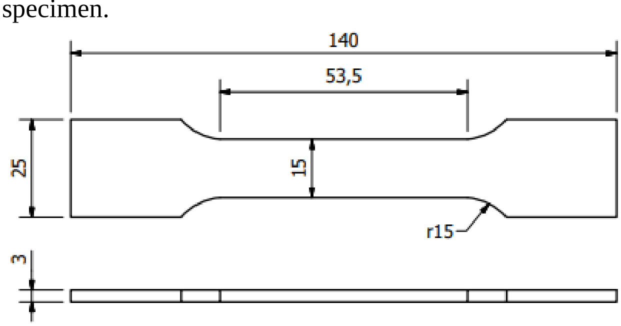

Fig 7. Dimensions of tensile test specimens

Mechanical strength testing with tensile test method on specimens was carried out using Universal Testing

Machine Tarno Grocki. Fig 8 explains the tensile test experiment process.

Fig 8. Tensile test process

Table 5 shows the impeller dimension parameters that are left constant as controlled variables in this experiment.

Table 5. Controlled Variables.

Parameters Dimension	Value
Radius impeller (mm)	19,5
Diameter Boos (mm)	15
Rood angle (◦)	36,6

Table 6 shows several rake length parameters that were varied to serve as independent variables in the experiment.

Table 6. Independent Variables impeller parameters.

Parameter	Low	Middle	High
Rake length (mm)	10	15	20

Three different impeller shape variations were obtained, which are presented as follows:

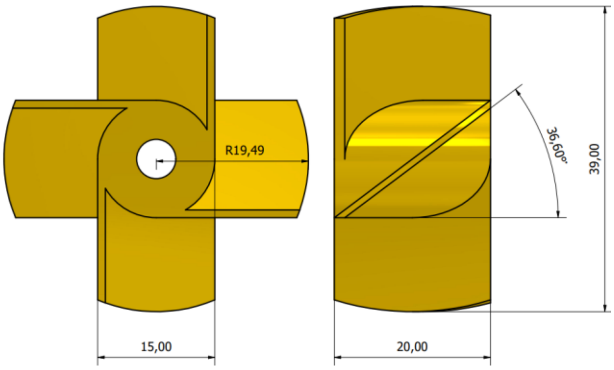

Fig 7. Impeller dimensions with a rake length of 20 mm.

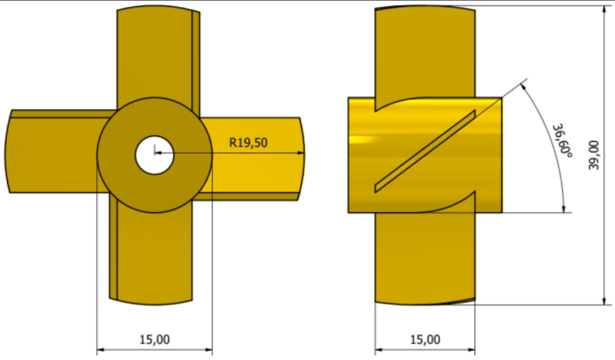

Fig 8. Impeller dimensions with a rake length of 15 mm.

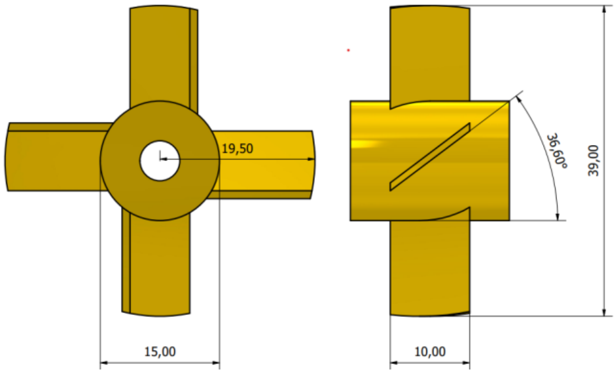

Fig 9. Impeller dimensions with a rake length of 10 mm.

The rake length of the impeller affects the fluid flow, which has a direct impact on the speed and thrust of the jet boat. The optimal rake length combination increases the flow efficiency, resulting in higher acceleration and maximum thrust. Conversely, an inappropriate rake length can cause turbulence and reduce thrust performance. Therefore, rake length is used as an independent variable in the study.

4. RESULT AND DISCUSION.

4.1 Tensile Test Results of ABS Specimens.

From the tensile test results using the JIS Z2201 standard, at 3D printing parameters with a layer height of 0.1 mm, 30% gyroid infill, and a speed of 40 mm/s. The maximum tensile stress reaches 24 Mpa. Fig 10 explains the strain and stress graphs of the tensile test results.

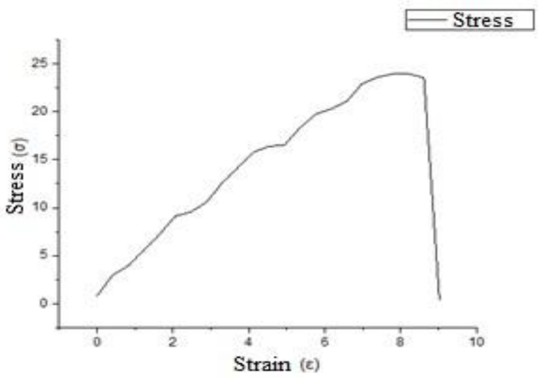

Fig 10. Stress and strain graph

Fig 10 illustrates the stress-strain relationship observed during the test. The graph highlights the material's elasticity and ultimate tensile strength, showing its capacity to withstand stress before deformation and failure. This combination of parameters provides a balance between print quality and mechanical performance, making it suitable for applications requiring moderate strength and precision.

4.2 Analysis of Impeller rake length 20 mm.

The distribution of stress concentration that occurs on the impeller with a rake length of 20 mm can be seen in Fig 11 as follows:

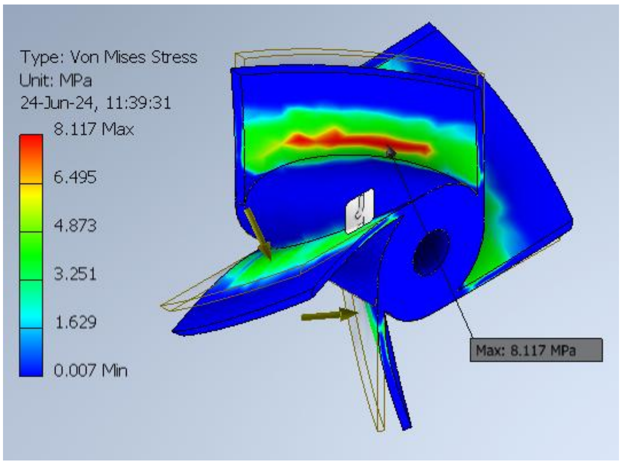

Fig 11. Simulation of stress concentration of impeller with rake length 20 mm.

From Fig 11, it can be explained the stress that occurs in the impeller body with a reke length of 20 mm. The stress that occurs in the Boos section is 1.62 Mpa, the stress that occurs in the Tip section is 1.62 Mpa, the stress that occurs in the Root section is 8.11 Mpa, the stress that occurs in the Face section is 4.87 Mpa, the stress that occurs in the Trailing edge section is 3.25 Mpa and the stress that occurs in the leading edge section is 3.25 Mpa. The simulation of the water flow rate that occurs in the impeller with a rake length of 20 mm reaches 562.01 cm/s. An illustration of the flow rate that occurs in the impeller can be seen in Fig 12 as follows:

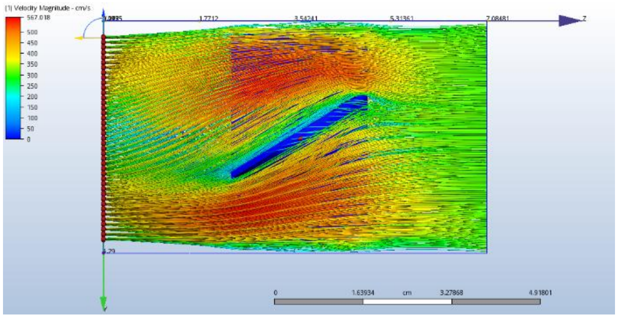

Fig 12. Simulation of flow rate on an impeller with a racket length of 20 mm.

From the simulation of the movement of the speed and pressure of the water flow that occurs in the impeller, it can be explained through the convergence plot graph in Fig 13 as follows:

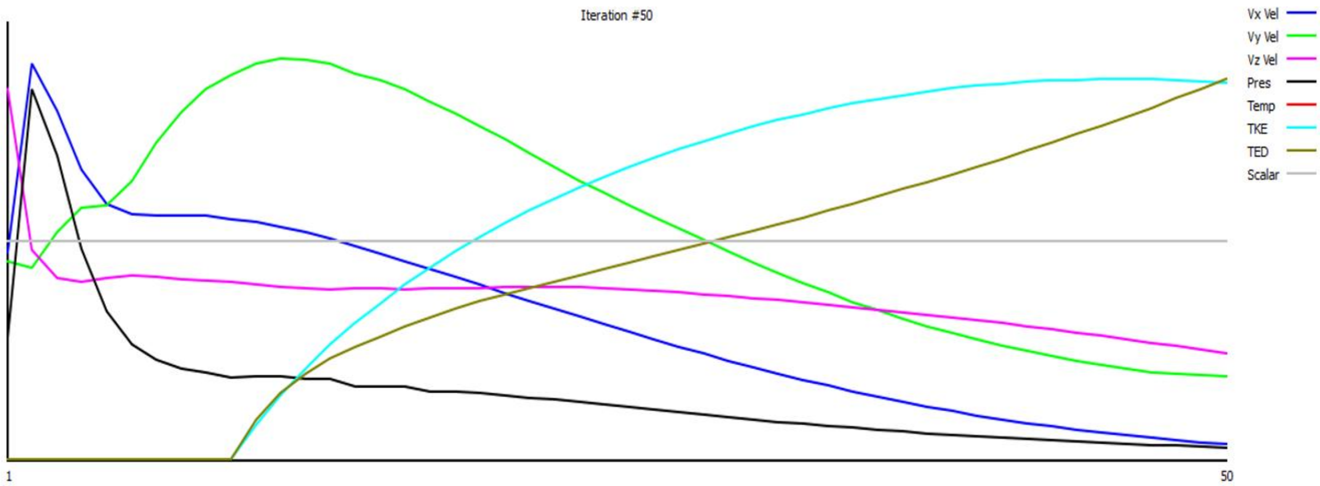

Fig 13. Convergence plot of water flow velocity and pressure.

From the convergence graph in Fig 13, it can be explained that the suction flow rate of the impeller with a rake length of 20 mm in the Inlet Duct area reaches 250 cm/s and the thrust flow rate of the impeller with a rake length of 20 mm in the Outlet Duct area reaches 567 cm/s.

4.3 Analysis of Impeller rake length 15 mm.

The distribution of stress concentration that occurs on the impeller with a rake length of 15 mm can be seen in Fig 14 as follows:

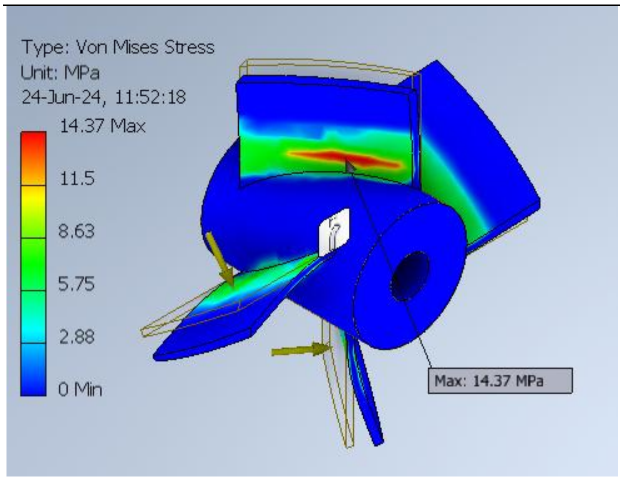

Fig 14. Simulation of stress concentration of impeller with rake length 15 mm.

Fig 12, it can be explained the stress that occurs in the impeller body with a reke length of 15 mm. The stress that occurs in the Boos section is 2.88 Mpa, the stress that occurs in the Tip section is 2.88 Mpa, the stress that occurs in the Root section is 14.37 Mpa, the stress that occurs in the Face section is 8.63 Mpa, the stress that occurs in the Trailing edge section is 5.75 Mpa and the stress that occurs in the leading edge section is 5.75 Mpa.

The simulation of the water flow rate that occurs in the impeller with a rake length of 15 mm reaches 571 cm/s. An illustration of the flow rate that occurs in the impeller can be seen in Fig 15 as follows:

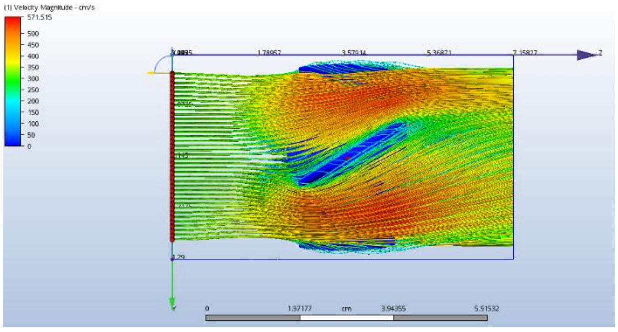

Fig 15. Simulation of flow rate on an impeller with a racket length of 15 mm.

The simulation of the movement of the speed and pressure of the water flow that occurs in the impeller, it can be explained through the convergence plot graph in Fig 16 as follows:

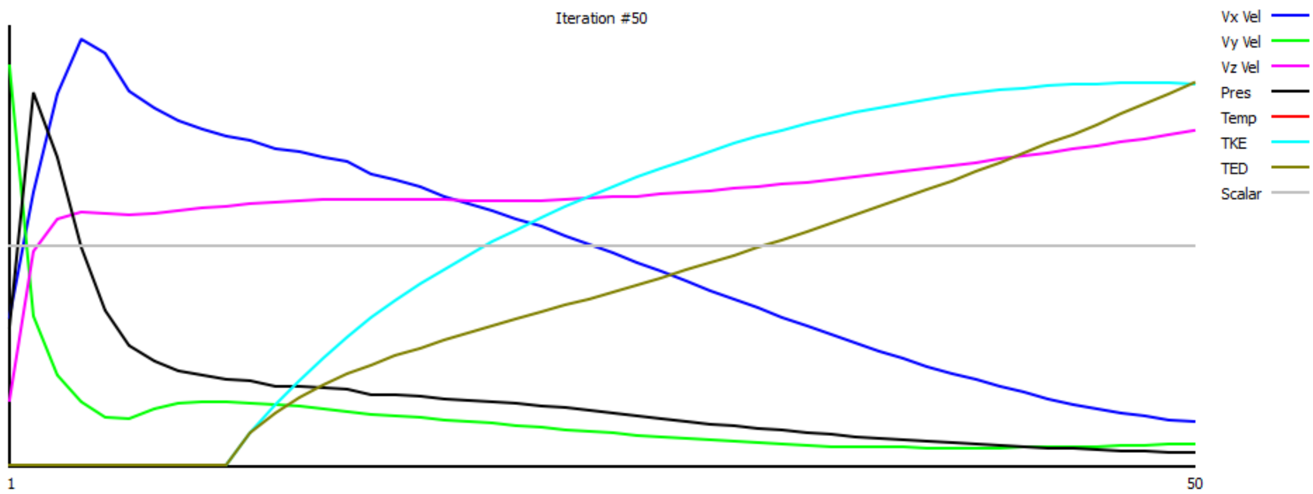

Fig 16. Convergence plot of water flow velocity and pressure.

From the convergence graph in Fig 16, it can be explained that the suction flow rate of the impeller with a rake length of 15 mm in the Inlet Duct area reaches 250 cm/s and the thrust flow rate of the impeller with a rake length of 15 mm in the Outlet Duct area reaches 571 cm/s

The distribution of stress concentration that occurs on the impeller with a rake length of 10 mm can be seen in Fig 17:

4.4 Analysis of Impeller rake length 10 mm.

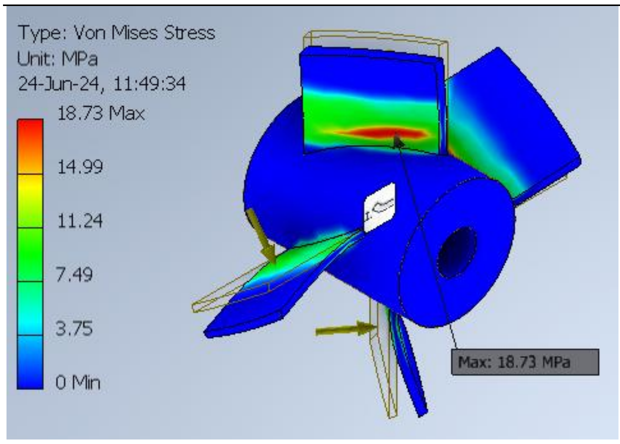

Fig 17. Simulation of stress concentration of impeller with rake length 10 mm.

Fig 17, it can be explained the stress that occurs in the impeller body with a reke length of 20 mm. The stress that occurs in the Boos section is 3.75 Mpa, the stress that occurs in the Tip section is 3.75 Mpa, the stress that occurs in the Root section is 18.73 Mpa, the stress that occurs in the Face section is 11.24 Mpa, the stress that occurs in the Trailing edge section is 7.49 Mpa and the stress that occurs in the leading edge section is 7.49 Mpa.

The simulation of the water flow rate that occurs in the impeller with a rake length of 10 mm reaches 562.01 cm/s. An illustration of the flow rate that occurs in the impeller can be seen in Fig 18:

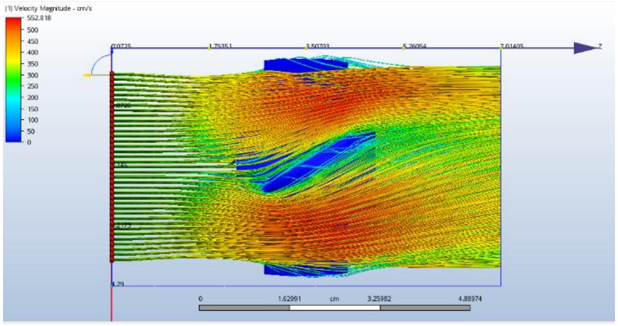

Fig 18. Simulation of flow rate on an impeller with a racket length of 10 mm.

The simulation of the movement of the speed and pressure of the water flow that occurs in the impeller, it can be explained through the convergence plot graph in Fig 19:

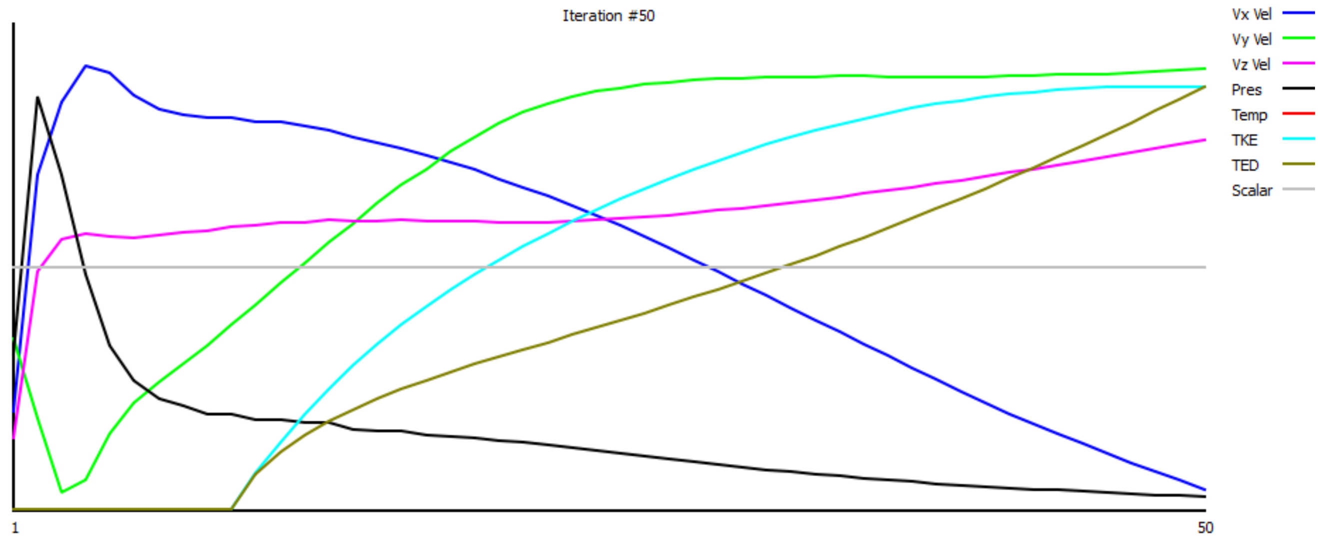

Fig 19. Convergence plot of water flow velocity and pressure.

the convergence graph in Fig 19, it can be explained that the suction flow rate of the impeller with a rake length of 10 mm in the Inlet Duct area reaches 250 cm/s and the thrust flow rate of the impeller with a rake length of 10 mm in the Outlet Duct area reaches 552.8 cm/s From the simulation results on the impeller with a combination of reke length 10m, 15mm, and 20mm. a diagram of the stress distribution that occurs in the impeller design that is designed when the impeller is working can be made. It can be seen in Fig 20

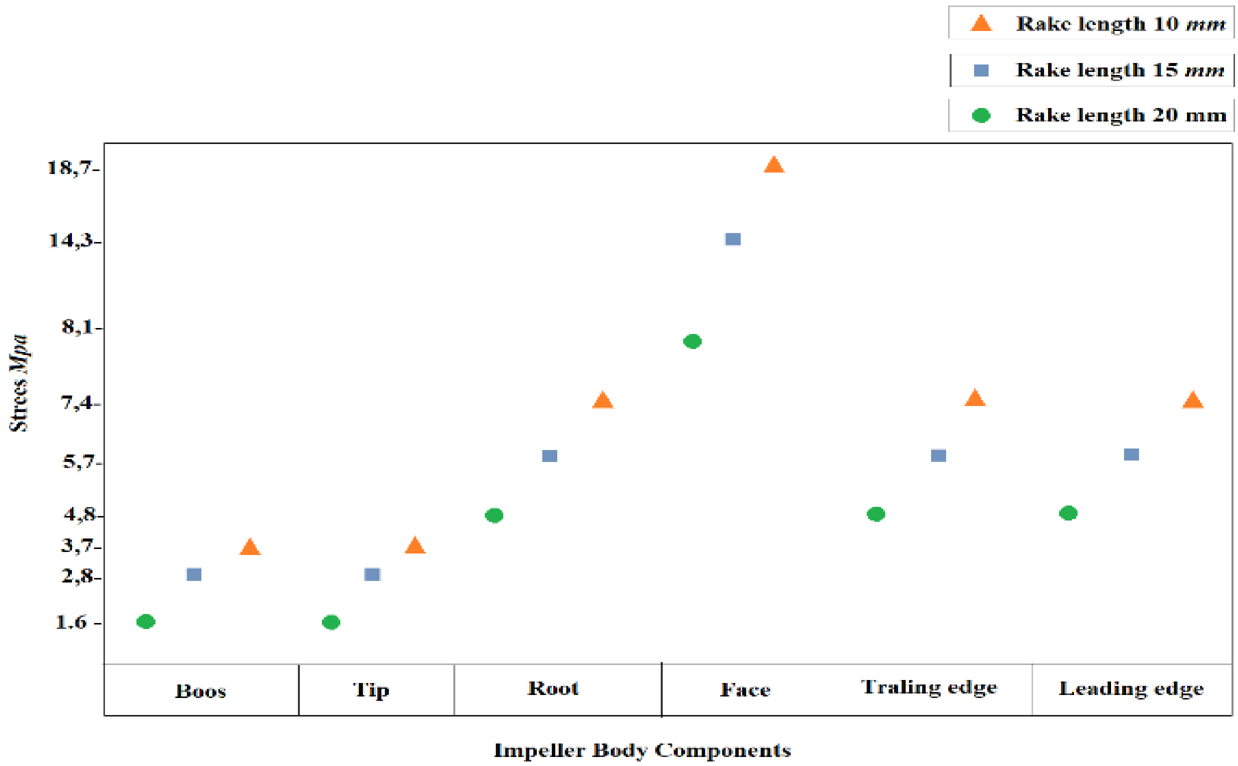

Fig 20. Stress distribution on the impeller body.

The fig 20 graph depicts the stress distribution across the various components of the impeller body for three rake lengths (10 mm, 15 mm, and 20 mm). The 10 mm rake length consistently shows higher stress values, peaking at 18.7 MPa at the “Face” component. In contrast, the 20 mm rake length shows the lowest stress values across all components, indicating lower efficiency in force transfer. The 15 mm rake length provides moderate stress values, indicating a balance between performance and structural integrity.

The results highlight that a shorter rake length (10 mm) results in higher stress transfer, which is important for applications requiring maximum thrust. Conversely, longer rake lengths reduce pressure, which can increase durability but at the expense of performance. This finding allows for tailored impeller designs for specific operational needs.

Compared to conventional methods that rely on empirical tuning, the proposed method integrates systematic parameter optimization, allowing for the analysis of stress distribution across the impeller components. This allows for the identification of the optimal rake length to maximize performance. Unlike previous studies, where stress data were generalized without detailed component details, this study provides insight into component-specific behavior.

5. CONCLUSIONS

The ideal parameters for printing ABS impellers with 3D printing are 0.1 mm layer height, 30% gyroid infill, with a speed of 40 mm/s. The maximum tensile stress reaches 24 Mpa. The impeller printing results are declared safe because the calculation results of the maximum impeller stress when working is 18.73 Mpa Where the safety factor (SF) value is 1.28

The recommended dimensions for the impeller are made with a rake length of 15 mm. with a stress distribution on the Boos section of 2.88 Mpa, Tip of 2.88 Mpa, Root of 14.37 Mpa, Face of 8.63 Mpa, Trailing edge of 5.75 Mpa and Leading edge of 5.75 Mpa. With the results of the simulation calculation of the water flow rate that occurs in the impeller reaching 571 cm / s.**6.**

ACKNOWLEDGEMENTS

I would like to express my deepest gratitude to all the participants who took part in this study. Their willingness to share their time and experiences has been essential in providing the data needed to carry out this research.

7. AUTHOR CONTRIBUTIONS

- Conceptualization: Lazuardi Lazuardi, Maryono Maryono.
- Data curation: Lazuardi Lazuardi , Maryono Maryono.
- Formal analysis: Muhammad Akhlis Rizza, Sugeng Hadi Susilo.
- Examination: Muhammad Akhlis Rizza, Sugeng Hadi Susilo.
- Methodology: Muhammad Akhlis Rizza, Sugeng Hadi Susilo

- Project administration: Maryono Maryono
- Source: Muhammad Akhlis Rizza, Sugeng Hadi Susilo.
- Software: Lazuardi Lazuardi.
- Supervisor: Sugeng Hadi Susilo.
- Validation: Muhammad Akhlis Rizza, Sugeng Hadi Susilo.
- Visualization: Lazuardi Lazuardi, Maryono Maryono.
- Writing – original draft: Lazuardi Lazuardi , Maryono Maryono.
- Writing – review & editing: Muhammad Akhlis Rizza, Sugeng Hadi Susilo.

8. REFERENCES

[1] J. W. Stansbury and M. J. Idacavage, "3D printing with polymers: Challenges among expanding options and opportunities," *Dent. Mater.*, vol. 32, no. 1, pp. 54-64, 2016.
[2] D. L. Bourell, M. C. Leu, and D. W. Rosen, "Roadmap for additive manufacturing: Identifying the future of freeform processing," *SME, Rapid Technologies and Additive Manufacturing*, vol. 5, pp. 1-14, 2009.
[3] L. Murr, "Metallurgy of additive manufacturing: Examples from electron beam melting," *Additive Manufacturing*, vol. 5, pp. 1-16, 2015.
[4] T. Wohlers and T. Caffrey, "Wohlers Report 2017: 3D printing and additive manufacturing state of the industry," *Wohlers Associates Inc.*, 2017.
[5] S. Sing, J. An, W. Y. Yeong, and F. E. Wiria, "Laser and electron-beam powder-bed additive manufacturing of metallic implants: A review on processes, materials and designs," *Journal of Orthopaedic Research*, vol. 34, no. 3, pp. 369-385, 2016.
[6] B. R. Munson, D. F. Young, and T. H. Okiishi, *Fundamentals of Fluid Mechanics*, 6th ed., New York, NY, USA: Wiley, 2009.
[7] J. A. Sparenberg, "Jet propulsion of a boat with a flexible stern flap," *Journal of Fluid Mechanics*, vol. 126, pp. 225-242, 1983.
[8] J. Carlton, *Marine Propellers and Propulsion*, 3rd ed., Oxford, UK: Butterworth-Heinemann, 2012.
[9] S. R. Turnock, "A performance study of marine waterjet propulsion systems," *Journal of Ship Research*, vol. 46, no. 2, pp. 102-112, 2002.
[10] J. M. Anderson and N. K. Chahine, "Jet thrusters for ship and boat propulsion: A review," *Ocean Engineering*, vol. 41, pp. 93-110, 2012.
[11] S. Turnock, "Performance prediction of marine waterjets," *Journal of Ship Research*, vol. 50, no. 2, pp. 128-137, 2006.
[12] L. Lazuardi, M. Akhlis Rizza, and M. Maryono, "Article Information ABSTRACT," *Journal of Evrimata: Engineering and Physics*, vol. 01, no. 02, pp. 61–69, 2023.
[13] C. Tropea, A. Yarin, and J. F. Foss, *Handbook of Experimental Fluid Mechanics*, New York, NY, USA: Springer, 2007.
[14] A. Tisa, P. 1∗, and B. Wahyudi, "Simulation Strength Analysis on PVC Pipe Blade Propeller Horizontal Axis Wind Turbine with Tip Elbow," *Journal of Evrimata: Engineering and Physics*, vol. 02, no. 01, pp. 78–84, 2024.
[15] P. Makridis and K. Brouwers, "Waterjet propulsor performance prediction," *Journal of Fluids Engineering*, vol. 130, no. 4, pp. 041301-041309, 2008.
[16] L. D. Knopper and C. A. Ollson, "Health effects and wind turbines: A review of the literature," 2011. [Online]. Available: http://www.ehjournal.net/content/10/1/78.
[17] M. Whitcomb and R. C. Huang, "Improved efficiency of waterjet propulsion with optimized nozzle design," *Ocean Engineering*, vol. 45, pp. 32-41, 2012.
[18] S. Pfaffel, S. Faulstich, and K. Rohrig, "Performance and reliability of wind turbines: A review," Energies, vol. 10, no. 11. MDPI AG, Nov. 01, 2017. doi: 10.3390/en10111904.
[19] P. J. Tavner, J. Xiang, and F. Spinato, "Reliability analysis for wind turbines," Wind Energy, vol. 10, no. 1, pp. 1–18, 2007, doi: 10.1002/we.204.
[20] L. Larsson and H. Raven, *Ship Resistance and Flow*, 2nd ed., New York, NY, USA: Wiley, 2010.
[21] S. Hadi Susilo, E. Yudiyanto, and B. Indra Kurniawan, "Simulation of Quadcopter Flying Electric Vehicle Chassis Article Information ABSTRACT," 2024.
[22] K. J. Maki, J. Katz, and P. Chang, "Waterjet propulsion: A review of recent developments," *Journal of Fluids Engineering*, vol. 133, no. 4, pp. 041301-041311, 2011.
[23] P. W. Roberts, "Automatic control for waterjet thruster systems," *IEEE Journal of Oceanic Engineering*, vol. 26, no. 4, pp. 562-572, 2001.
[241]N. Shahrubudin, T. C. Lee, and R. Ramlan, "An overvi ew on 3D printing technology: Technological, materials, and applications," in Procedia Manufacturing, Elsevier B.V., 2019, pp. 1286–1296. doi: 10.1016/j.promfg.2019.06.089.
[25] L. Lazuardi, M. Akhlis Rizza, S. H. Susilo, and M. Maryono, "ANALYSIS OF 3D PRINTING APPLICATIONS WITH ABS FILAMENT MATERIAL FOR DESIGNING UNMANNED AIRCRAFT BODYBUILS Article Information ABSTRACT," *Journal of Mechanical Engineering*, vol. 01, no. 01, pp. 25–32, 2024.
[26] A. I. Cooper, "3D printing in the laboratory: Maximize material properties with minimal effort," *Nature Reviews Materials*, vol. 1, pp. 150-153, 2017.
[27] A. T. Gaynor and J. K. Guest, "Topology optimization considering overhang constraints: Eliminating sacrificial support material in additive manufacturing through design," *Structural and Multidisciplinary Optimization*, vol. 54, no. 5, pp. 1157-1172, 2016.
[28] M. L. Griffith et al., "Understanding the microstructure and performance of components

fabricated using laser engineered net shaping," *Journal of Materials Research*, vol. 13, no. 10, pp. 2843-2852, 1998.

[29] S. H. Masood, "Advances in fused deposition modeling," *Comprehensive Materials Processing*, vol. 10, pp. 69-91, 2014.

[30] I. Gibson, D. W. Rosen, and B. Stucker, *Additive Manufacturing Technologies*, 2nd ed., New York, NY, USA: Springer, 2015.

[31] I. Gibson, D. W. Rosen, and B. Stucker, Additive manufacturing technologies: Rapid prototyping to direct digital manufacturing. Springer US, 2010. doi: 10.1007/978-1-4419-1120-9.

[32] Z. Ali, E. B. Türeyen, Y. Karpat, and M. Çakmakci, "Fabrication of Polymer Micro Needles for Transdermal Drug Delivery System Using DLP Based Projection Stereo-lithography," in Procedia CIRP, Elsevier B.V., 2016, pp. 87–90. doi: 10.1016/j.procir.2016.02.194.

[33] M. Frascio, E. A. de Sousa Marques, R. J. C. Carbas, L. F. M. da Silva, M. Monti, and M. Avalle, "Review of tailoring methods for joints with additively manufactured adherends and adhesives," Materials, vol. 13, no. 18. MDPI AG, Sep. 01, 2020. doi: 10.3390/ma13183949.

[34] V. Petrovic, J. Vicente Haro Gonzalez, O. Jordá Ferrando, J. Delgado Gordillo, J. Ramon Blasco Puchades, and L. Portoles Grinan, "Additive layered manufacturing: Sectors of industrial application shown through case studies," Int J Prod Res, vol. 49, no. 4, pp. 1061–1079, Feb. 2011, doi: 10.1080/00207540903479786.